Syntheses and Characterization of Lithium Alkyl Mono- and Dicarbonates as Components of Surface Films in Li-Ion Batteries

ARTICLE *in* THE JOURNAL OF PHYSICAL CHEMISTRY B · MAY 2006

Impact Factor: 3.3 · DOI: 10.1021/jp0601522 · Source: PubMed

7 AUTHORS, INCLUDING:

Kang Xu
Army Research Laboratory
175 PUBLICATIONS **5,679** CITATIONS
SEE PROFILE

Shengshui Zhang
Army Research Laboratory
169 PUBLICATIONS **5,865** CITATIONS
SEE PROFILE

Philip N Ross
University of California, Berkeley
360 PUBLICATIONS **21,401** CITATIONS
SEE PROFILE

Richard Jow
Army Research Laboratory
170 PUBLICATIONS **4,892** CITATIONS
SEE PROFILE

Syntheses and Characterization of Lithium Alkyl Mono- and Dicarbonates as Components of Surface Films in Li-Ion Batteries

Kang Xu,*,† Guorong V. Zhuang,‡ Jan L. Allen,† Unchul Lee,† Sheng S. Zhang,† Philip N. Ross, Jr.,‡ and T. Richard Jow†

Electrochemistry Branch, Sensors and Electron Devices Directorate, U. S. Army Research Laboratory, Adelphi, Maryland 20783-1197, and Materials Sciences Division, Lawrence Berkeley National Laboratory, Berkeley, California 94720

Received: January 9, 2006; In Final Form: February 22, 2006

A homologous series of lithium alkyl mono- and dicarbonate salts was synthesized as model reference compounds for the frequently proposed components constituting the electrolyte/electrode interface in Li-ion batteries. The physicochemical characterization of these reference compounds in the bulk state using thermal analyses and X-ray photoelectron, nuclear magnetic resonance, and Fourier transform infrared spectroscopies establishes a reliable database of comparison for the studies on the surface chemistry of electrodes harvested from Li-ion cells.

Introduction

Since the birth of Li-ion battery technology, it has been recognized that the selection of electrolyte solvents plays a critical role in the reversibility of the cell chemistry.[1] Through electrochemical reduction of the electrolyte solvent molecules during the initial cycles, a new solid interface is formed on graphitic anode surfaces. This interface is believed to be a dense layer that has the properties of an electrolyte, i.e., permeable only to Li^+ migration while impervious to electron tunneling. It is this solid electrolyte interface (SEI) that sustains the reversible Li^+ intercalation−deintercalation chemistry within the graphite lattice. In state-of-the-art Li-ion batteries, organic esters of the carbonic acid family are almost exclusively used as electrolyte solvents, as a result of their combined properties of ion solvation, electrochemical stability, and, above all, the ability to form a stable and protective SEI layer.[2] Often known as dialkyl (linear) or alkene (cyclic) carbonates, these solvents include dimethyl carbonate (DMC), diethyl carbonate (DEC), ethylmethyl carbonate (EMC), ethylene carbonate (EC), and propylene carbonate (PC). The exact electrolyte formulations used in commercial Li-ion devices usually remain trade secrets and differ with manufacturers, cell chemistries, as well as intended applications; nevertheless, the invariable part of all these formulations is the cyclic carbonate EC in mixture with one or more linear carbonates selected from DMC, EMC, and DEC. The presence of the other cyclic carbonate, PC, is rather limited due to its tendency to exfoliate the graphene layer structure of anodes.[2] Accordingly, one of the most active areas of Li-ion battery research during the past decade has been the study of electrochemical reduction of the above organic esters.[2−5]

The well-established mechanism of the surface reduction for cyclic carbonates has been the single-electron reduction pathway proposed by Aurbach et al. (Scheme 1), which leads to the commonly named alkyl carbonates or semi-carbonates in the general form of **I**.[3,4]

SCHEME 1: Proposed Single-Electron Mechanism for the Reduction of Alkene (Cyclic) Carbonates

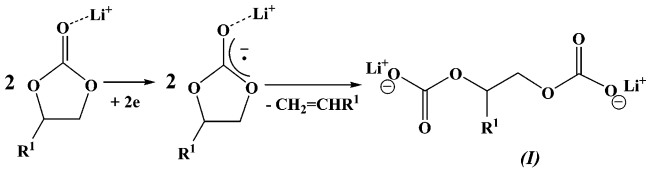

$R^1 = H$ (EC) or CH_3 (PC)

Aurbach et al. later went further to suggest that it was due to the presence of one particular alkyl dicarbonate in the SEI, i.e., lithium ethylenedicarbonate (LEDC) which forms upon the reduction of EC, that graphitic carbonaceous materials could be used as the negative host (anode) for Li^+.[5] This seminal notion predated the fact learned later that EC is the indispensable solvent in all electrolyte compositions and hence has been well accepted by the electrochemical community. When Ein-Eli found that unary electrolytes based on DMC and EMC were also able to support reversible Li-ion chemistry with graphitic anodes, the above single-electron pathway was naturally extended to these dialkyl (linear) carbonates (Scheme 2).[6] The formed mono-lithium salts of the alkyl carbonates with the structure of **II** are presumed to possess similar physicochemical properties as LEDC.

The above lithium alkyl mono- and dicarbonates (**I** and **II**), with selected alkyl structures, are believed to act as the essential passivating ingredients in the SEI and therefore constitute the very foundation of Li-ion chemistry, despite the fact that their physicochemical properties in the bulk state remain to be characterized, and their reliable spectroscopic identification on actual electrode surfaces has not been established. One of the difficulties encountered in this research effort has been the absence of commercially available reference compounds to assist in the interpretation of spectral data obtained from graphite anodes after SEI formation, e.g., infrared vibrational[7] or X-ray photoelectron spectra.[8] In an effort to gain fundamental under-

* Author to whom correspondence should be addressed. E-mail: cxu@arl.army.mil.
† U. S. Army Research Laboratory.
‡ Lawrence Berkeley National Laboratory.

10.1021/jp0601522 CCC: $30.25
Published on Web 03/29/2006

SCHEME 2: Single-Electron Mechanism Extended to the Reduction of Dialkyl (Linear) Carbonates

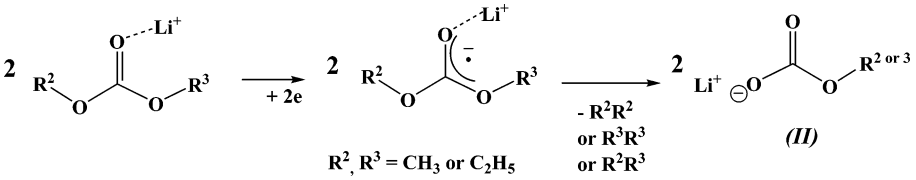

SCHEME 3: Model Compounds LMC, LEC, LEDC, and LPDC, as Postulated Reduction Products from DMC, EMC, DEC, EC and PC, Respectively, via the Single-Electron Reduction Process on the Graphitic Anode Surface[a]

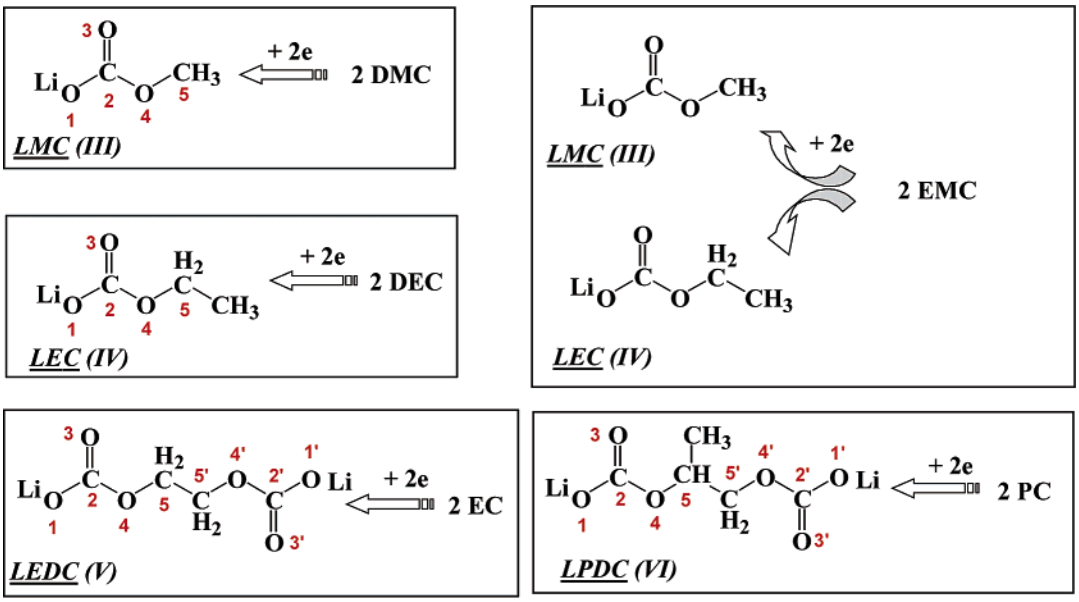

[a] The atoms are numerically labeled for functionality identification in the discussion of FTIR spectra.

standing on these key ingredients in the SEI, at the U. S. Army Research Laboratory (ARL), we synthesized a series of model lithium alkyl carbonate compounds to simulate the proposed chemical species on the anode surfaces within state-of-the-art Li-ion devices. The syntheses started in early 2004, while part of the characterization was carried out in collaboration with the team at Lawrence Berkeley National Laboratory (LBNL).[9,10] A similar effort was carried out by a French team[11,12] at about the same time, who share the common belief with us that the study of these authentic alkyl carbonate compounds will be of significance to decipher the laws governing Li-ion chemistry.

In this paper, we present the syntheses and physicochemical characterization of a homologous series of alkyl carbonates, which serve as model products of the proposed electrochemical reduction of EC, PC, DMC, EMC, and DEC, respectively: lithium methyl carbonate (LMC), lithium ethyl carbonate (LEC), lithium ethylene dicarbonate (LEDC), and lithium propylene dicarbonate (LPDC), as summarized in Scheme 3.

Experimental Section

In view of the extreme sensitivity of the targeted compounds toward ambient moisture, the entire process of synthesis and workup were conducted in a dry room with dew point below −85 °C (corresponding to H_2O < 1 ppm), and a rigorous drying procedure was followed for all of the starting materials and reagents. Typically, the alcohols (methanol, ethanol, ethylene glycol, and propyl-1,2-diol) were repeatedly dried over 3 Å molecular sieves that have been activated at 400 °C, followed by redistillation until the moisture level was less than 10 ppm, as determined by Karl Fischer titration (Mettler-Toledo). All of the deuterated NMR solvents went through the same procedures without redistillation.

NMR samples were sealed in ground-jointed glass tubes under Ar until analysis, so that the incursion of ambient moisture can be kept to a minimum. NMR analyses were conducted at the NMR facility at the University of Maryland using either a 400 MHz Oxford or a 500 MHz Bruker spectrometer. Tetramethylsilane (TMS) was used as either an internal or an external reference to determine the chemical shifts. Fourier transform infrared (FTIR) spectroscopy measurements were performed at the LBNL in attenuated total reflection (ATR) mode at a resolution of 4 cm^{-1} with a total of 512 scans. Due to the high sensitivity of these compounds toward ambient moisture, sample handling and measurement were under a He environment. The experimental procedures in handling air-sensitive samples have been described in a previous publication.[13]

X-ray diffraction (XRD), X-ray photoelectron spectroscopy (XPS), and thermal gravimetric analysis (TGA) were conducted at the ARL. The XRD patterns were collected on a Rigaku Ultima III diffractometer using the parallel beam method with Cu Kα radiation (λ = 1.5418 Å) and scanning from 5° to 60° (2θ). Prior to data collection, samples were loaded onto glass slides and hermetically covered with Kapton film in the argon-filled glovebox. Indexing of the patterns was attempted using the TREOR90 program.[14] Preliminary scans of all four salts revealed a pattern with dominant peaks that are orders of magnitude stronger in intensity than others. To rule out a preferred orientation effect both symmetric ($2\theta/\theta$ scan) and asymmetric scans with the X-ray source fixed at 2.5° were conducted. No gross changes in the diffraction patterns were

SCHEME 4: Dumas−Peligot Synthesis of Alkali Metal Alkyl Carbonates

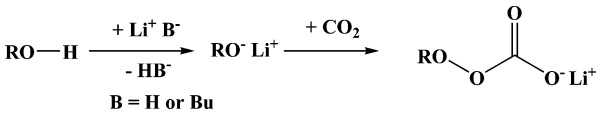

observed, thus eliminating the possibility that samples are oriented on the sample plates, an artifact introduced during the sample loading.

For XPS analyses the powdery samples of the salts were immobilized on carbon tabs, which were then loaded into the analysis chamber using a vacuum sample transporter. During the whole process the samples were either exposed only to Ar atmosphere (dew point < -85 °C) or under high vacuum ($<10^{-10}$ bar). Surface analysis was then conducted with a PHI 5800 XPS system, where an Mg Kα excitation source was used. The energy resolution is about 0.3 eV, and the binding energy scale is calibrated to the binding energy of the C 1s core for amorphous carbon at 284.3 eV. Studies on the thermal stability of these four salts were carried out with a Perkin-Elmer TGA-7 analyzer. Typically the samples were loaded under a dry N_2 atmosphere, and the heating rate was kept at 5 °C/min from room temperature up to 550 °C under a steady stream of nitrogen.

Results and Discussion

Syntheses. The general synthetic routes were modified from that of Dumas and Peligot,[15] and they consisted of two stages: (1) conversion of alcohols into corresponding lithium alkoxides and (2) nucleophilic attack of alkoxides on carbon dioxide.

Both Aurbach et al.[3] and Tarascon et al.[11] adopted routes similar to those in Scheme 4, although different lithiating agents were employed. We initially used lithium hydride (LiH, 95%, Aldrich) and found that it works well for methanol and ethanol because these parent alcohols in excess can conveniently serve as solvents and their high volatility made them readily removable in the purification process. After lithiation, the analytic grade CO_2 was directly introduced into the alcoholic solutions of lithium alkoxides, after passing through one gas column packed with 3 Å molecular sieves and two bubblers containing 98% concentrated sulfuric acid. The reactions for both methoxide and ethoxide were exothermic, and white flake crystals precipitated almost instantly in the solution, with the reactant mixture becoming nearly neutral from strongly alkaline. After more than 3 h of CO_2 treatment and filtration, the crystals were collected and washed repeatedly with dried methanol or ethanol, followed by drying under vacuum ($<10^{-2}$ Torr) for at least 48 h at room temperature. The final isolation yields were 88% and 82% for LMC and LEC, respectively. According to the nomenclature recommended by the International Union of Pure and Applied Chemistry (IUPAC), these two compounds should be named *2-oxa-propanoic acid lithium salt* (**III**) and *2-oxa-butanoic acid lithium salt* (**IV**). Instead, the abbreviations of their common names (LMC and LEC, respectively) will be used throughout the text.

The reactions of LiH with the two diols (ethylene glycol and propane-1,2-diol), however, were rather sluggish, most likely due to their higher viscosity. This reduced activity caused concerns that the complete lithiation of both hydroxyl groups in the same molecule might be very unlikely if an excess amount of the diols were used. We suspect that, consequently, a mixture consisting of the targeted dialkoxides and monoalkoxides with one unreacted alcohol functionality would be obtained instead. Moreover, the high boiling points of these diols (~200 °C) made them prohibitively difficult to remove once the treatment of CO_2 is completed.

To cope with these complications, we adopted a stronger lithiating agent, *n*-butyllithium (*n*-BuLi, 2.5 M solution in hexane, Aldrich), for the diols to ensure a complete alkoxide conversion. The diols were thus added dropwise, under vehement stirring and a dry nitrogen stream, to a stoichiometric amount of *n*-BuLi solution diluted by anhydrous diethyl ether. The resultant dialkoxides were then isolated, dried, and suspended in dry acetonitrile (AN) for carbonization. With vehement stirring, analytic grade CO_2 was introduced into the suspension. The reaction was not obviously exothermic, perhaps due to the lower reactivity of the dialkoxides as compared with their monofunctional counterparts, but the appearance of the reactant gradually changed from the turbid suspension of fine powder (dialkoxides) to a clear solution with visible white crystal flakes. The obtained crystals were washed repeatedly with dry AN and then vacuum-dried at room temperature under 10^{-2} Torr for 48 h. The final isolation yields in this work were 67% and 78% for LEDC and LPDC, respectively. The IUPAC names for these dilithium salts should be *2,5-oxa-hexane-1,6-dioic acid dilithium salt* (**V**) and *2,5-oxa-3-methyl-hexane-1,6-dioic acid dilithium salt* (**VI**), respectively.

Structural Identification. The structural identification of these synthesized lithium alkyl carbonates was mainly conducted by means of $^1H/^{13}C$ NMR spectra (ARL) and FTIR (LBNL).

Since these four salts are barely soluble in any common NMR solvents, to obtain their structure information in aprotic media, we adopted the strategy of suspending these salts in the polar deuterated solvents such as acetone (AC-d_6), dimethyl sulfoxide (DMSO-d_6), or acetonitrile (AN-d_3), in the hope that the saturated solutions of the samples—no matter how low their concentrations are in the solutions—could generate sufficient signal level under the prolonged shimming and data acquisition. The strategy proved rather effective, as Figures 1−5 demonstrate. Typically, after as long as 20 h of data acquisition in a 400 MHz magnetic field, even the most elusive sp^2-hybridized carbons (the carbonyl functionality in the carbonates) can provide satisfactory ^{13}C spectra with a signal-to-noise ratio higher than 3.0. Table 1 tabulated all of the chemical shifts of the salts determined in NMR measurements.

Figure 1 shows the ^1H and ^{13}C NMR collected from the suspension of the synthesized LMC in AC-d_6. The absence of a proton signal for H_2O, which should be located at around 2.8 ppm in this solvent, confirms that the drying procedure is effective in removing trace amounts of moisture. [16] The ^1H signal at 3.56 ppm (singlet, for C**H**$_3$−O−) as well as ^{13}C signals at 62.401 ppm (singlet, for **C**H$_3$−O−) and 160.97 ppm (singlet, for −**C**(O)−) are consistent with the structure of **III**. The absence of other ^1H and ^{13}C nuclei indicates the adequate purity of the sample. The ^1H and ^{13}C NMR of the above salt were also collected from its suspension in DMSO-d_6, as shown in Figure 2. The effect of NMR solvent on the general appearance of the spectra seemed to be negligible other than that both ^1H and ^{13}C signals shifted to high field; i.e., for C**H**$_3$−O− the signal shifted from 3.56 to 3.27 ppm, while for **C**H$_3$−O− and −**C**(O)− from 62.401 and 160.97 ppm to 51.513 and 157.02 ppm, respectively. Perhaps because LMC is more soluble in DMSO-d_6 than in AC-d_6, the sp^2-hybridized carbonyl generates a C^{13} signal of much higher abundance relative to solvent signals in this case. The general features of the spectra remained despite the solvents, indicating a consistent and stable structure.

TABLE 1: Chemical Shifts of ^{1}H and ^{13}C Nuclei in the Four Lithium Alkyl Mono- and Dicarbonates

lithium alkyl carbonates	^{1}H (ppm)	^{13}C (ppm)
LMC	3.56 (s, AC-d_6); 3.27 (s, DMSO-d_6)	62.40 (AC-d_6), 160.97 (AC-d_6); 51.51 (DMSO-d_6), 157.02 (DMSO-d_6)
LEC	1.051(t, 3H), 3.502 (q, 2H)	15.02, 57.55, 160.07
LEDC	3.53 (s)	157, 62.9
LPDC	1.101 (d, 3H), 3.51−3.37 (o, 2H), 3.853−3.81 (m, 1H)	17.87, 66.83, 66.48, 160.49

[a]The deuterated solvents used are indicated in parentheses.

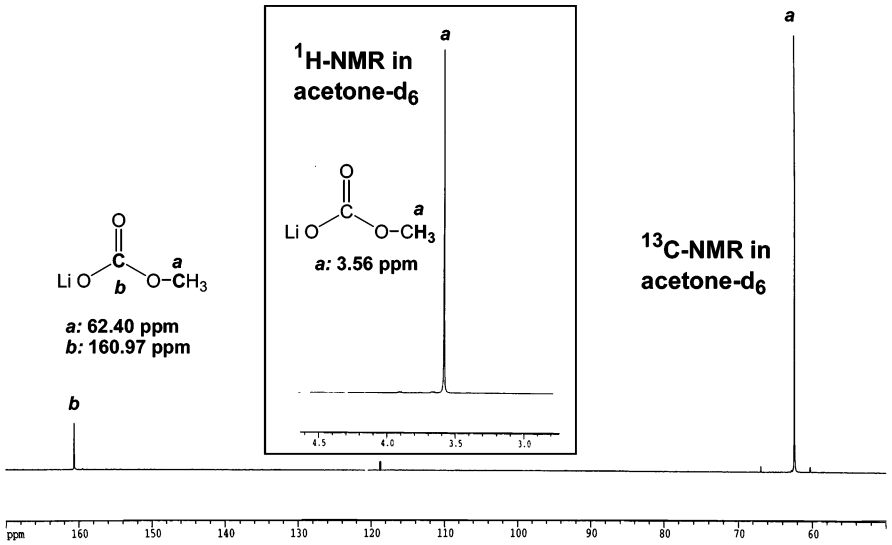

Figure 1. ^{1}H and ^{13}C NMR spectra of the synthesized lithium methyl carbonate (LMC), the proposed reduction product of DMC through a single-electron mechanism. The spectra were collected in AC-d_6 with asterisks marking the solvent signals arising from the proton residuals due to incomplete deuteration.

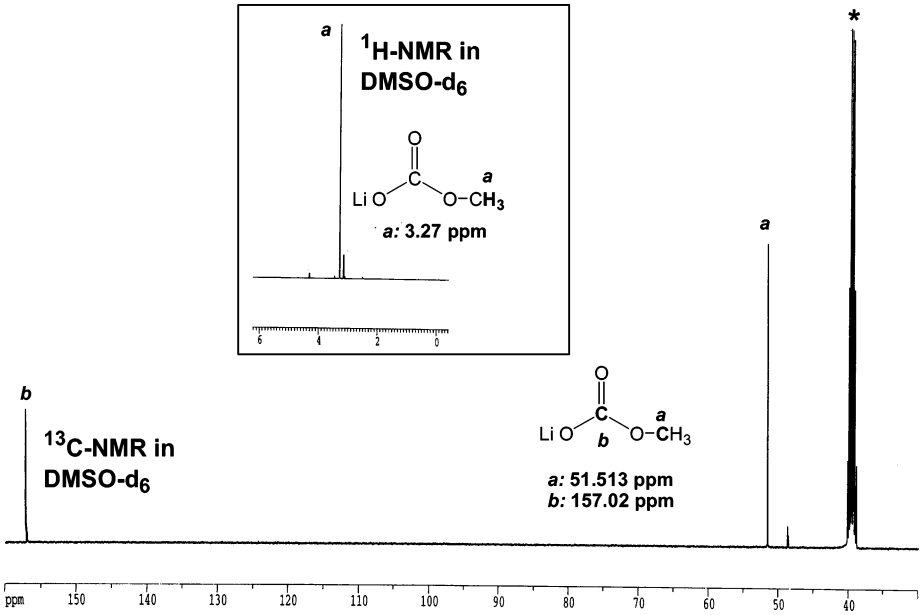

Figure 2. ^{1}H and ^{13}C NMR spectra of the synthesized lithium methyl carbonate (LMC) collected in DMSO-d_6 with asterisks marking the solvent signals arising from the proton residuals due to incomplete deuteration.

Figure 3 shows the ^{1}H and ^{13}C NMR spectra collected from the suspension of the synthesized LEC in AC-d_6. The ^{1}H signals at 1.051 ppm (triplet, for C**H**$_3$−CH$_2$−) and 3.502 ppm (quartet, for CH$_3$−C**H**$_2$−O−) are consistent with both the chemical shift and the split pattern of a substructure CH$_3$−CH$_2$−O−, whose further proof comes from the integration of these signals, which produces a proton ratio of 3:2 (not shown in the figure). Like LMC, the proof of the existence of carbonyl comes from the ^{13}C spectrum, which shows a conspicuous peak at 160.07 ppm. The other two ^{13}C nuclei detected have chemical shifts at 15.02 ppm (for **C**H$_3$−CH$_2$−) and 57.55 ppm (for CH$_3$−**C**H$_2$−), corresponding to the substructure CH$_3$−CH$_2$−O−.

Figure 4 shows the ^{1}H and ^{13}C NMR collected from the suspension of the synthesized LEDC in AC-d_6. The highly symmetric structure of LEDC results in rather simple spectra for both ^{1}H and ^{13}C nuclei. Thus, there is only one ^{1}H signal at 3.53 ppm (for −O−C**H**$_2$−C**H**$_2$−O−), while only two ^{13}C signals at 62.9 ppm (for −O−**C**H$_2$−**C**H$_2$−O−) and 157 ppm (for −O−**C**O$_2$−), respectively. Especially, the lower abundance of the ^{13}C signals as compared with the other salts seems to

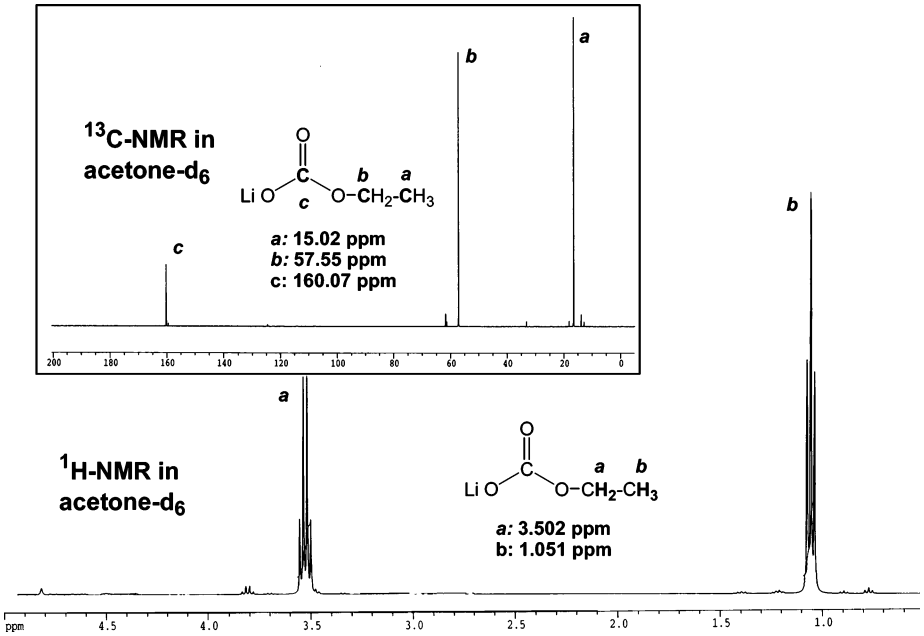

Figure 3. ^{1}H and ^{13}C NMR spectra of the synthesized lithium ethyl carbonate (LEC), the proposed reduction products of DEC—and also one of the products of EMC—through a single-electron mechanism.

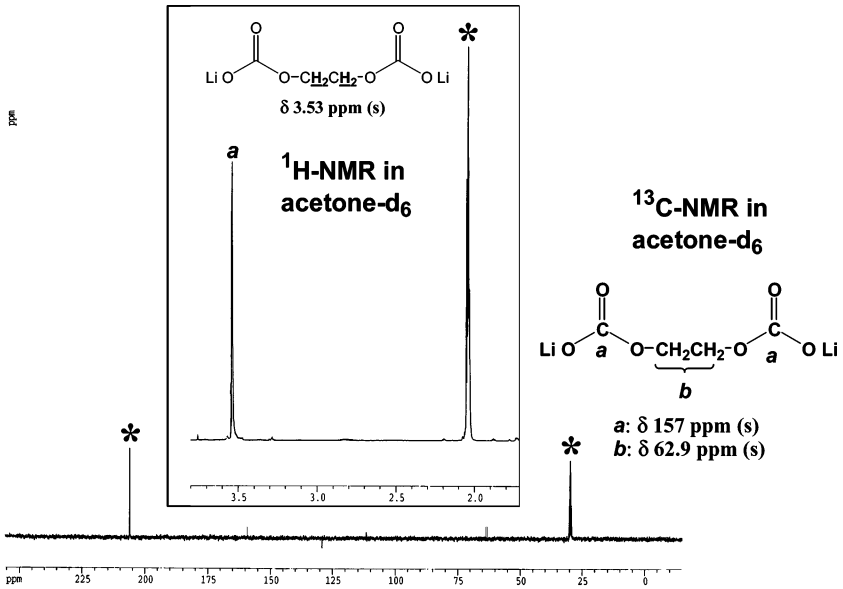

Figure 4. ^{1}H and ^{13}C NMR spectra of the synthesized lithium 1,2-ethylene dicarbonate (LEDC), the proposed reduction product of EC through a single-electron mechanism. The spectra were collected in AC-d_6 with asterisks marking the solvent signals arising from the proton residuals due to incomplete deuteration.

indicate a particularly low solubility in this solvent, considering that a similar duration of data acquisition was applied to all samples. This property may have a significant consequence on the behavior of this salt in battery electrolyte and will be discussed later.

Figure 5 shows the ^{1}H and ^{13}C NMR collected from the suspension of the synthesized LPDC in AN-d_3. The presence of a methyl branch in the alkyl moiety breaks the molecular symmetry and complicates the spectra. The doublet at 1.10 ppm for C**H**$_3$− indicates a C**H**$_3$−CH− substructure, while the multiplets between 3.37 and 3.81 ppm represent a characteristic split pattern of the −O−C**H**(CH$_3$)−C**H**$_2$−O− as already observed in PC or 2-methyl-propane-2,3-diol. [16,17] Integration of peak area further confirms the above substructure with a proton ratio of 3:1:2. ^{13}C NMR detected four nonisotropic ^{13}C nuclei, which are located at 17.87 ppm (for **C**H$_3$−), 66.50 ppm (for −O−**C**H$_2$−), 67.8 ppm (for −O−**C**H(CH$_3$)−), and 160.50 ppm (for −**C**(O)−), respectively. In comparison with the ^{13}C NMR of the PC molecule, [17] the relative abundance of the sp^2-hybridized carbon peak (at 160.50 ppm) in LPDC is obviously much higher, indicating a much enriched carbonyl content in the molecule (two carbonyls) versus its parental molecule PC (one carbonyl).

The FTIR spectra of LMC, LEC, LPDC, and LEDC are presented in Figures 6A and 6B, and Table 2 summarizes the characteristic vibrational frequencies and their corresponding group frequency assignments. For better comparison, the spectra in Figure 6 are normalized with respect to the strongest peak at 1652 cm^{-1} in LMC. In the 2000−700 cm^{-1} region, common to all of the lithium alkyl mono- and dicarbonates are three group frequencies in the spectral regions marked by a, b, and c. The first vibrational mode a is characteristic of the delocalized

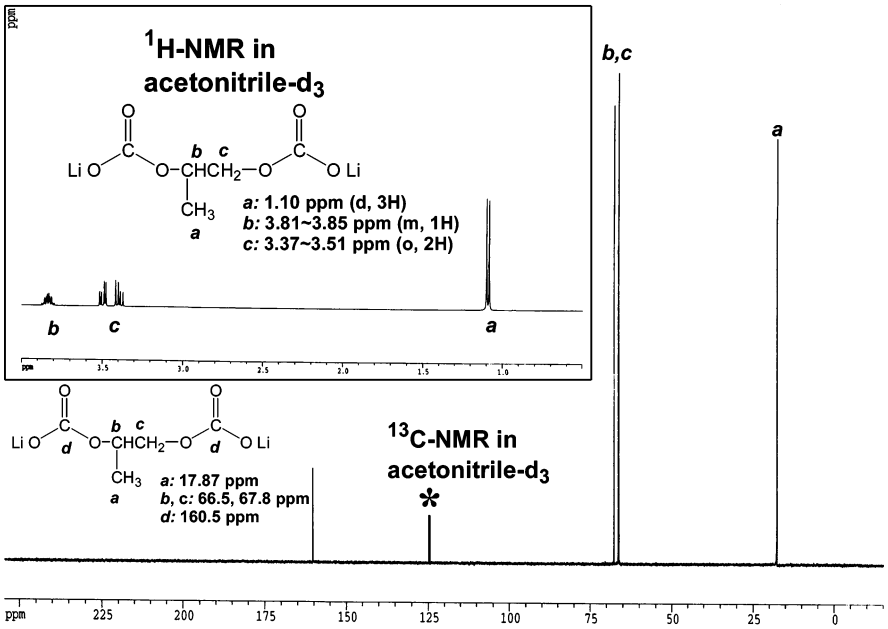

Figure 5. ^{1}H and ^{13}C NMR spectra of the synthesized lithium 1,2-propylene dicarbonate (LPDC), the proposed reduction product of PC through a single-electron mechanism. The spectra were collected in AN-d_3 with asterisks marking the solvent signals arising from the proton residuals due to incomplete deuteration.

TABLE 2: Characteristic Vibrational Frequencies (cm^{-1}) of LMC, LEC, LEDC, and LPDC and Their Group Frequency Assignments

group frequency assignment	LMC	LEC	LEDC	LPDC
alkyl and alkenes	3017, 2996		3006	2991
(asymmetric or symmetric stretchings)		2982, 2973	2976	2977
	2961		2962	
		2929	2944	2941
		2909	2909, 2887	2909, 2889
	2869	2875		
O(1)C(2)O(3)	1653	1642, 1615	1662, 1652	1660, 1652
(asymmetric stretchings)	1480, 1466, 1452	1416	1402	1422, 1399
	1374, 1351	1376	1386	1378
				1353
		1331	1317, 1304	1303
C(2)O(4)C(5) (asymmetric stretchings)	1097	1104	1116	1113
O(1)C(2)O(3)O(4) (out-of-plane bendings)	822	836	825	828

carbonyl group O(1)C(2)O(3) asymmetric stretching, while the second vibrational mode b at ca. 1100 cm^{-1} is attributed to the C(2)O(4)C(5) asymmetric stretching mode. The vibrational mode c originates from the carbonate group O(1)C(2)O(3)O(4) out-of-plane bending. These group frequencies were confined to a rather narrow range of $\sim$20 cm^{-1}, which is relatively independent of whether the salt is a mono- or dicarbonate. The vibrational frequency and peak shape of the delocalized carbonyl group O(1)C(2)O(3) in LEDC and LPDC are very similar in that both have a peak at ca. 1662 cm^{-1} with a slightly asymmetric shape due to the presence of a shoulder at a lower wavenumber. However, the vibrational frequency of the corresponding carbonyl group in the two mono alkyl carbonates (LEC and LMC) is shifted down by about 10 wavenumbers. Moreover, what distinguishes LEC from LMC is the single O(1)C(2)O(3) peak of LMC at 1643 cm^{-1} versus the two distinctive peaks of LEC at 1616 cm^{-1}. Such peak splitting in LEC is an indication of the different chemical environment of O(1)C(2)O(3) in the highly crystalline phase (bulk phase). It is expected that such distinctive peak splitting might not be observed in an SEI layer as formed in an actual Li-ion cell, where LEC is expected to coexist with amorphous species/phases in the surface film.

Aside from the group frequencies unique to both mono- and dialkyl carbonates, the spectral features associated with other functional groups also allow us to differentiate the four alkyl carbonates. As shown in Figure 6B, methyl, ethyl, ethylene, and 1,2-propylene groups in those compounds exhibit characteristic asymmetric and symmetric stretching modes, which reflect combinations of various methyl (CH_3), ethyl (CH_3CH_2), methane (CH), ethoxy (OCH_2), and methoxy (OCH_3) groups in the 3000$-$2800 cm^{-1} region. Some of those functional groups would also give rise to reliable bending and deformation modes, while others have only fingerprints in the 1500$-$1300 cm^{-1} spectral regions. For example, the CH_2 wagging mode in alkene dicarbonates (LEDC and LPDC) gives rise to medium strength vibrational modes at ca. 1300 cm^{-1}. However, this mode is shifted to 1331 cm^{-1} in LEC as a result of coupling with the CH_3 symmetric deformation mode in LEC. Because of its relatively strong intensity in comparison with other vibrational modes, this mode serves as a fingerprint for mono- and dialkyl carbonates.

Thus, combining the spectroscopic information furnished by both NMR and FTIR, we conclude with confidence that these four compounds that are of interest to Li-ion battery chemistry have been obtained by us with high purity, and their structures

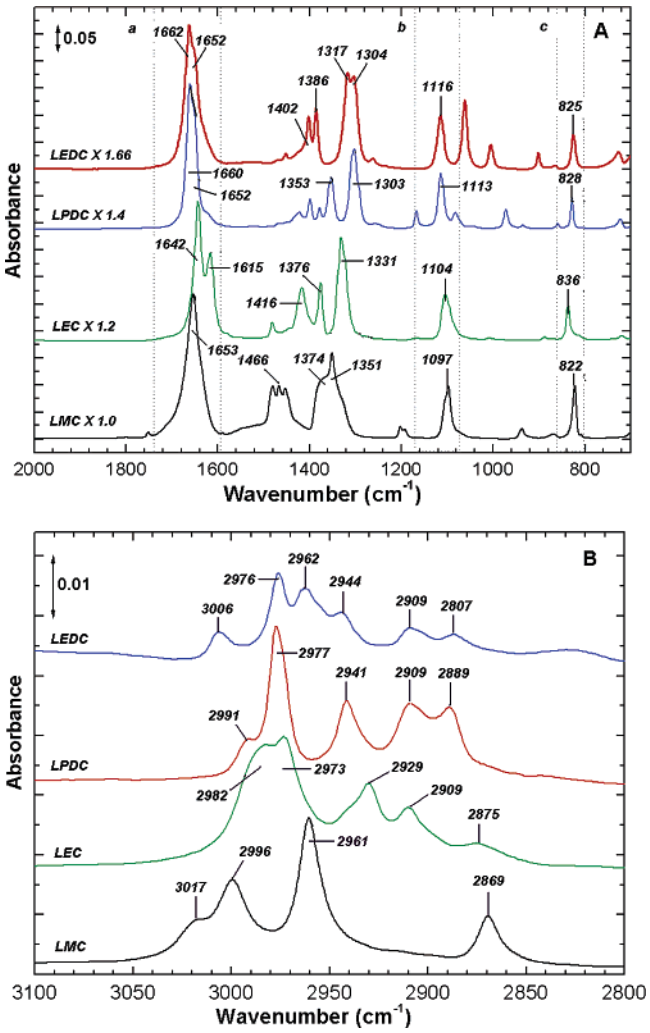

Figure 6. FTIR spectra for lithium alkyl mono- and dicarbonates: (A) group frequencies between 700 and 2000 cm^{-1} and (B) additional spectral features between 2800 and 3100 cm^{-1}. The spectra are normalized with respect to the strongest peak at 1652 cm^{-1} in LMC, and scaling factors are as marked.

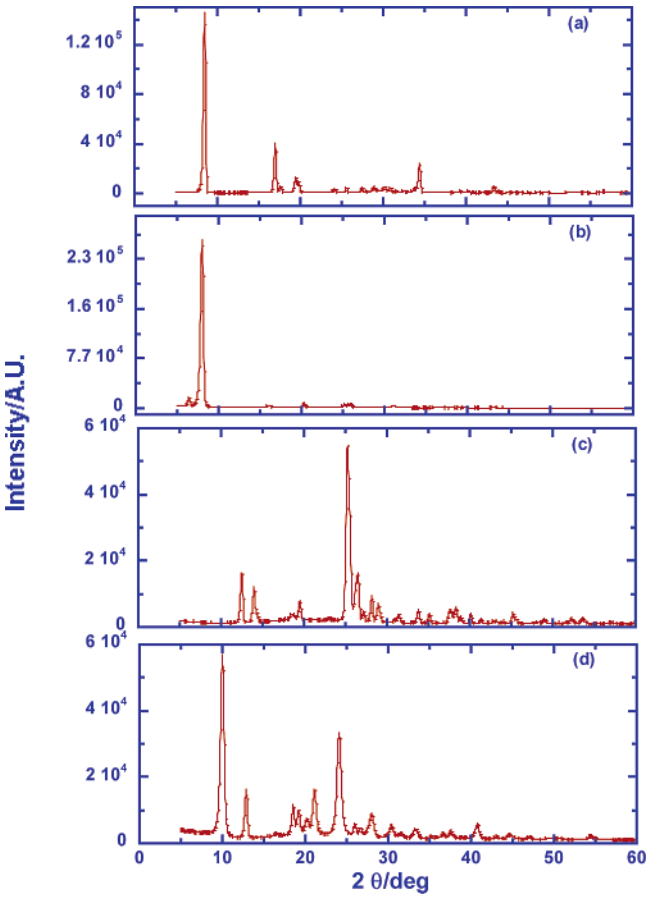

Figure 7. XRD patterns of the lithium alkyl mono- and dicarbonates: (a) LMC, (b) LEC, (c) LEDC, and (d) LPDC.

are consistent with the expected structures of **III**−**VI** as shown in Scheme 3.

More information about the bulk structure of these salts can be extracted from the X-ray diffraction experiments, as shown in Figures 7a−d. In all cases, the less-than-sharp widths of the diffraction peaks are characteristic of samples with small crystal sizes, which most probably arise from the insolubility of these lithium salts in the organic solvents employed during their syntheses, because, upon formation, these salts tend to immediately precipitate from the solution, thus denying the opportunity for the crystallite growth and resulting in very fine particles. The diffraction pattern of LMC (Figure 7a) shows one dominant peak at $2\theta = 8.50°$, which corresponds to a *d*-spacing of 10.4 Å. The next two peaks in order of intensity are at $2\theta = 17.00°$ and 34.38°, corresponding to 5.22 and 2.61 Å, respectively. Since these three *d*-spacings are approximately multiples following the above order, these reflections should be related. We were unable to index this pattern using TREOR90.[14] The diffraction pattern of LEC (Figure 7b) shows a dominant peak at $2\theta = 8.04°$ ($d = 10.99$ Å). The pattern could be indexed with a monoclinic lattice of $a = 14.11$ Å, $b = 5.24$ Å, and $c = 14.00$ Å, and $\beta = 103.22°$. All 13 lines were indexed, and the de Wolff figure of merit (FOM)[18] was 15. Since a general rule concerning the interpretation of diffraction data is that if at least the first 20 lines are indexed with the FOM being greater than 9, then the indexing is complete,[19] the criteria were not met, and the indexing is therefore not certain considering that we only had 13 lines available to index. The LEDC pattern (Figure 7c) could be indexed to an orthorhombic unit cell with lattice constants of $a = 14.100$ Å, $b = 12.66$ Å, and $c = 5.20$ Å. The de Wolff FOM was 10 based on 20 lines indexed; however, there was one line at $2\theta = 37.6°$ that could not be indexed. The diffraction pattern of LPDC (Figure 7d) shows the strongest reflection at $2\theta = 10.01°$ ($d = 8.79$ Å). We were unable to index this pattern to an acceptable FOM. In general, the monocarbonates (LMC and LEC) demonstrated higher crystallinity than the dicarbonates, which can also be observed in the FTIR spectra.

Figure 8a shows the X-ray photoelectron spectra for the C 1s core level in the four lithium alkyl carbonates, all of which demonstrate rather similar spectral features consisting of a conspicuous −C(O)O− functionality at the characteristic binding energy of 289 eV. While 284−285 eV signals were generated by the sample substrate that contains elemental carbon, the oxygen-containing species at ∼286 eV are also clearly discernible, which obviously should be assigned to alkoxide linkages in the salts. In general, the C 1s spectra shown in Figure 8a bear little resemblance to spectra obtained from an SEI on a carbon anode well-cycled in EC-based electrolyte, despite the same X-ray photospectrometer and handling procedure.[8] It is obvious that in the actual anodes harvested from an Li-ion cell there is a much lower abundance of the carbonyl functionality as compared with the presence of the $-CH_2O-$ functionality. In other words, the conspicuous peak at ∼286 eV as observed on the actual anode surface[8] does not arise from an integral

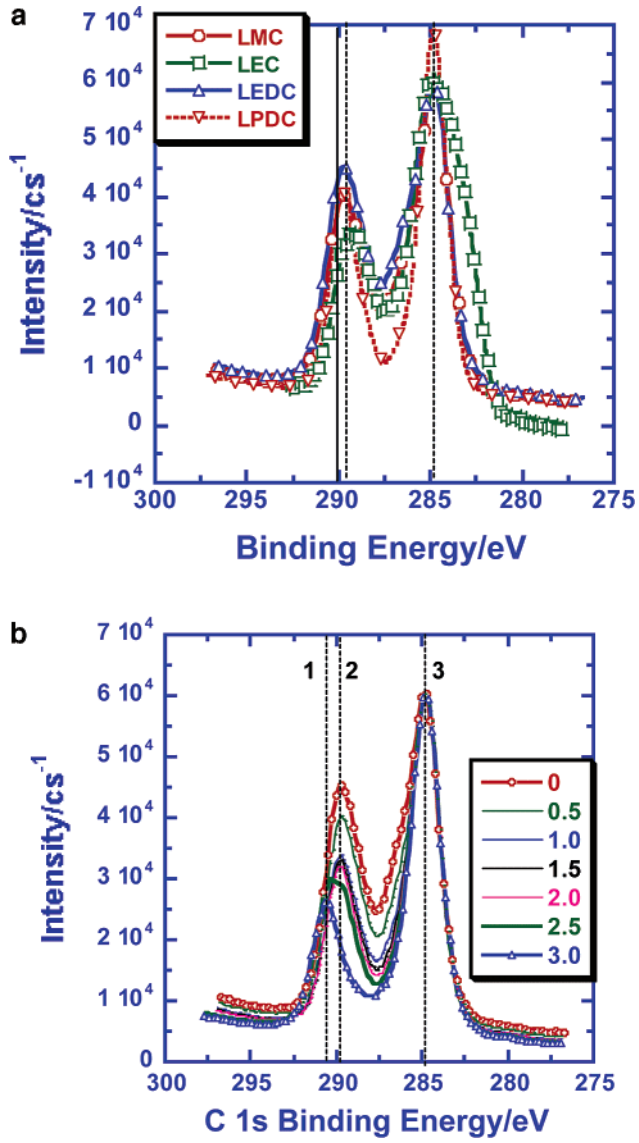

Figure 8. X-ray photoelectron spectroscopy for lithium alkyl mono- and dicarbonates: (a) C 1s spectra as normalized against the 284.5 eV peak in LMC; (b) the transformation of lithium alkyl carbonates to lithium carbonates due to their sensitivity toward ambient moisture.

part of the structure (i.e., the alkoxide linkage) within these lithium alkyl mono- or dicarbonates; instead, it might correspond to a high abundance of oligomeric species consisting of an ether linkage. As a logical conclusion from the above observations, these authentic lithium alkyl mono- and dicarbonates synthesized in this work should not be the exclusive chemical species existing in SEI.

Physical and Chemical Properties. As an effective barrier against continuous electrolyte reduction, the SEI in a working Li-ion cell must maintain its physical integrity on a graphitic anode against both simple dissolution and chemical erosion from the acidic electrolyte solutions. We tested the solubility of these four model lithium alkyl mono- and dicarbonates in a collection of nonaqueous solvents and found that they are essentially insoluble in dialkyl and alkene carbonates, carboxylic esters, alcohols, and ethers. The only exception is *N*,*N*′-dimethylformamide (DMF), which can dissolve LPDC up to 0.4 m and form a clear solution.

To further test the chemical stability of these salts, which are slightly basic in nature, toward the common electrolyte solutions, we placed these four synthesized salts in 1.0 m $LiPF_6$ in EC/DMC (1:1 by weight) and 1.0 m $LiBF_4$ in EC/DMC (1:1 by weight), respectively. No obvious change can be observed even after an accelerated aging process by storage at 60 and 75 °C for days. The salt crystals, which remained as white precipitates in the solutions, were recovered by filtration and subsequent washing with DMC. NMR analyses indicate no obvious structural change. Thus, it could be concluded that these alkyl carbonate salts are essentially inert toward not only the dissolution by the solvents but also the reactions with salt anions PF_6^- and BF_4^-, which are acidic in nature.

SCHEME 5: Inactivity of the Commonly Used Li Salts toward the Alkyl Carbonates and the Attack of the Corresponding Lewis Acids BF_3 and PF_5

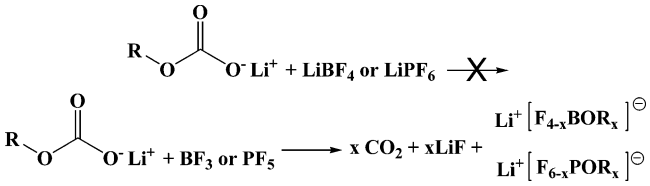

SCHEME 6: Moisture Sensitivity of Lithium Alkyl Carbonates

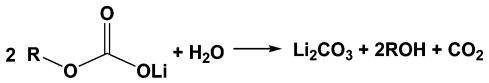

Despite the above observations, instability of these lithium alkyl carbonates was found when they are in the presence of the Lewis acids that constitute the commonly used lithium salts in Li-ion batteries. For example, adding the dimethyl etherate of BF_3 to any of these salts results in violent generation of CO_2, leaving behind a white precipitate that is confirmed by F 1s of XPS to be mainly composed of LiF (Scheme 5). We postulate that the basic nature of these alkyl carbonate salts makes them susceptible to attack from the strong Lewis acids, although these same salts are stable against the electrolyte solutions, because the Lewis acid cores in either $LiBF_4$ or $LiPF_6$ have been partially neutralized as the result of the coordination from the Lewis base LiF. By analogy, we believe a similar reactivity should exist when PF_5 is present.

Another species that should be considered is HF, which is known to universally exist in $LiBF_4$- and $LiPF_6$ -based electrolytes due to the reaction between the labile B−F or P−F bonds with trace moisture. Since the generation of HF and those Lewis acids might very likely be accelerated by elevated temperatures,[20] the instability of alkyl carbonates implies the vulnerability of SEI in an aged cell, where the SEI components are very likely to be corroded, calling for renewal formation and resulting in higher cell impedances, or simply cease to function as the protection of carbonaceous anodes.

It has been well-known since the pioneering work of Aurbach et al. that these lithium alkyl carbonates are extremely sensitive to moisture,[5] although their counterparts with other alkaline cations such as barium and potassium may form stable aqueous solutions or even monohydrate crystals.[15] This dependence of salt chemical stability on cation species is often encountered for lithium salts, the most conspicuous example being $LiPF_6$ versus RN_4PF_6 and $NaPF_6$, while quantum computation has indicated that Li^+ serves as an unique destabilizing agent for the anions toward moisture.[20] The decomposition mechanism of these alkyl carbonate anions has been suggested to lead to carbonate anions with CO_2 generation (Scheme 6).[21] Although, given the slight basic nature of these salts in aqueous solutions, we believe that what is more likely to be formed would be the

SCHEME 7: Alternative Path for the Moisture-Sensitive Lithium Alkyl Carbonates

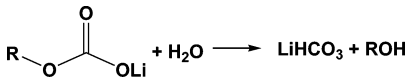

mixture of carbonate and bicarbonate anions with reduced gas production (Scheme 7).

Thus, it seems very likely that the ratio of moisture to salt determines whether Scheme 6 or 7 would be followed. In a real life scenario of an Li-ion cell electrode being exposed to ambient moisture, the moisture-limit mechanism of Scheme 6 should represent the dominant process, leaving Li_2CO_3 as the main species, which has been detected by various surface analytical means.[21,22] Previous observations of bicarbonate anion in aged cells with the presence of moisture seemed to be in support of the above speculations.[7]

To evaluate the moisture sensitivity of the lithium alkyl carbonate in a more quantitative manner, we conducted the ambient-exposure test on the LEDC sample immobilized on a carbon tab and monitored the shift in the binding energy of C 1s electrons in the carbonyl functionality. The relative humidity in the air-conditioned lab lies between 20% and 30%, and the duration of each exposure is kept at 30 s. As Figure 8b shows, with the exposure elapsed from 2 up to 3 min, the C 1s core spectra corresponding to the carbonyl group, located at 289 eV and characteristic of an alkyl carbonate structure as shown in **I** or **II**, experienced a gradual shift toward >290 eV, which is characteristic of carbonate (CO_3^{2-}) in nature. A simultaneous change during this shift is the gradual decrease in the relative abundance of the above C 1s signal, indicating the loss of the sp^2-hybridized carbonyl moiety in the population. It is immediately obvious that the above two changes detected by XPS should match the hydrolysis chemistry as described by Scheme 6, as there is no carbonyl loss in the mechanism represented by Scheme 7.

The state-of-the-art Li-ion cells suffer gradual but permanent loss in both capacity and power at temperatures above 60 °C, while hazardous thermal runaway occurs at 150 °C and above.[2] The cause for the degradation and failure at these elevated temperatures had been attributed to the deterioration of the bulk electrolyte components;[23] however, we are inclined to believe that the break down of SEI under those conditions should play a more decisive role, which would trigger a series of inter-reactions between the cell components such as active agents in the anode and the cathode, inert agents such as the binder and the conductive additives, and, especially, electrolytes.[2] Thermodynamically, all organic carbonate esters or salts tend to release CO_2 at high temperatures; therefore, if the SEI does indeed consist of the suggested lithium alkyl mono- or dicarbonates shown in Scheme 3, such a surface film would expectedly disintegrate under the sheer act of heat, i.e., even without the corrosive byproducts from the bulk electrolyte components. The presence of these undesired species, though, might very likely accelerate the tendency of generating CO_2.

In related studies on the thermal stability of Li-ion cells using differential scanning calorimetry (DSC) and accelerating rate calorimetry (ARC), a thermal event, starting at 120 °C and peaking at 140 °C, was observed with graphitic anodes harvested from Li-ion cells and had been identified as the decomposition of the SEI ingredients formed in the state-of-the-art electrolytes based on EC.[24,25] In an effort to correlate the thermal profiles obtained above with the bulk thermal stability of the potential SEI ingredients synthesized in this work, we monitored the

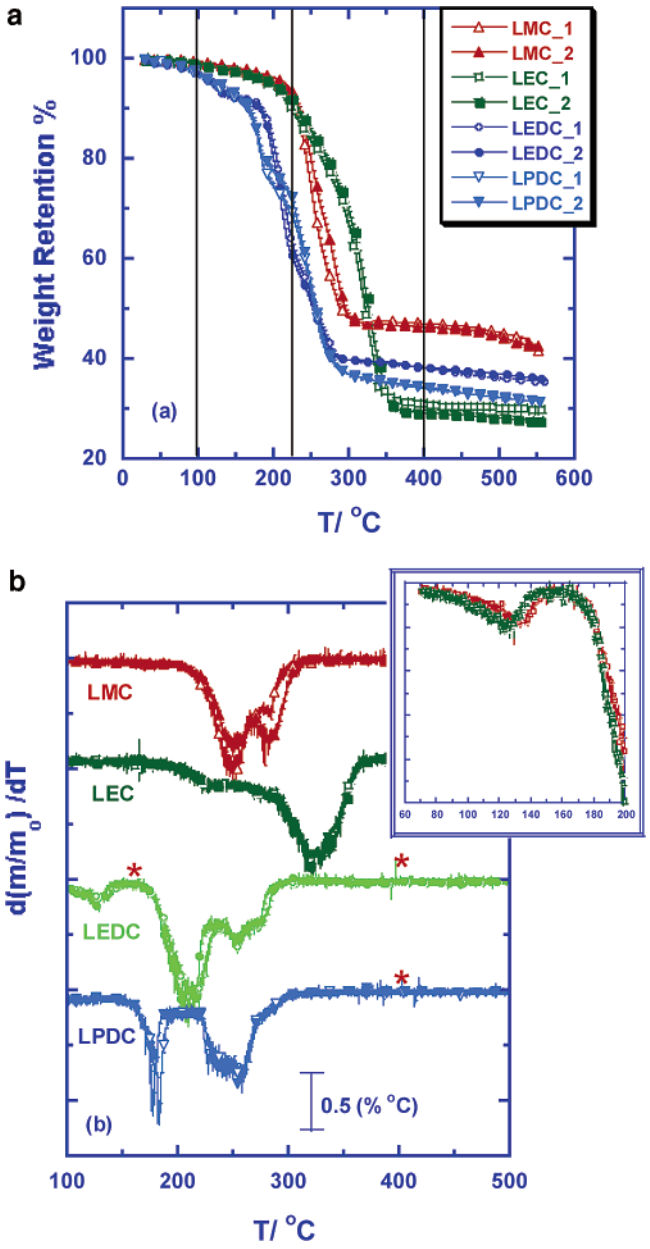

Figure 9. Thermal instability of the lithium alkyl carbonates: (a) weight retention as function of temperature as recorded with TGA; (b) onset temperatures of the multistaged thermal decompositions as demonstrated by DTG plots. The measurements were done with duplicate samples. Asterisks marked the temperatures where XPS and NMR analyses of the remnant were carried out. Inset: The onset event of LEDC decomposition.

weight loss of these four alkyl carbonates in the temperature range of 30−550 °C with TGA. For each alkyl carbonate duplicate experiments were conducted to ensure consistency, which, as indicated by Figure 9a, appeared to be excellent with standard deviations within 2%. To accurately locate the onset temperatures and to reveal the multiplicity of the thermal events, the derivative thermogravimetric (DTG) quantity $d(m/m_0)/dT$ was also plotted against temperature in Figure 9b. Apparently, the two mono-alkyl carbonates (LMC and LEC) exhibited much higher thermal stability than the two dicarbonates (LEDC and LPDC). The major weight losses of the latter two start at ~150 °C with the maximum weight loss at or below 200 °C, which are lower than the two monocarbonate salts by 60−100 °C. Obviously, for both mono- and dicarbonate salts multiple thermal processes with different onset temperatures exist,

TABLE 3: Weight Retentions of the Four Lithium Alkyl Mono- and Dicarbonates as Predicted from Schemes and Experimentally Measured

lithium alkyl carbonates	Schemes 8a and 8b	Schemes 9a and 9b	Schemes 10a and 10b	experimentally measured
LMC	45.05	46.27	18.29	42.10
LEC	38.47	54.12	15.53	28.55
LEDC	45.61	45.61	18.41	35.58
LPDC	41.97	49.94	16.95	31.35

SCHEME 8: Proposed Thermal Decomposition of Lithium Alkyl Carbonates Leading to Li_2CO_3

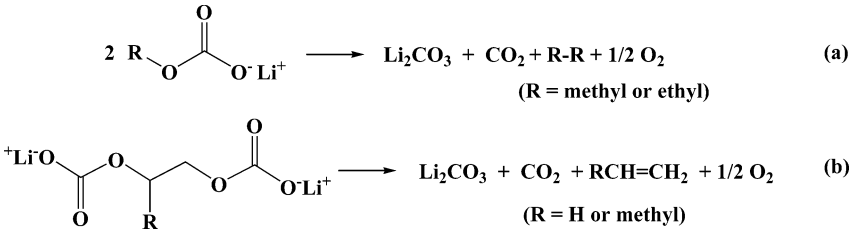

SCHEME 9: Proposed Thermal Decomposition of Lithium Alkyl Carbonates Leading to Alkoxides

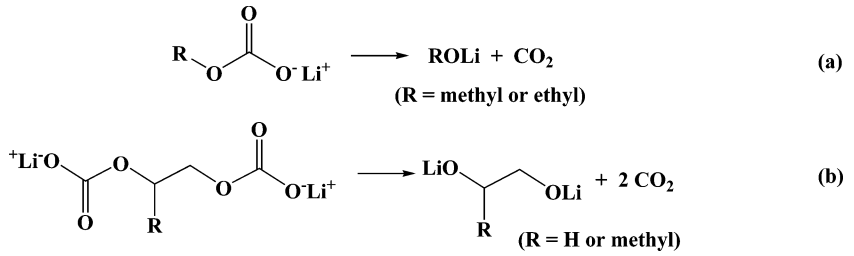

indicating a complicated thermal chemistry that very likely involves a competitive mechanism.

Of particular interest is the onset temperature of LEDC decomposition. Shown in Figure 9b and its inset is an event, small in magnitude but reproducible, between 120 and 130 °C, which seems to match the event claimed to be responsible for the break down of the SEI.[24,25] However, the major thermal processes of LEDC at higher temperatures (180−230 °C) were not clearly reflected in those DSC and ARC studies. One likely explanation for this discrepancy is that, in those DSC/ARC studies on graphitic anodes, the major thermal events occurring near 200 °C—such as the reaction between the lithiated carbon (LiC_6) and the polymer binder—are in such high magnitudes that any subsequent process of the alkyl carbonates in the SEI would be essentially concealed.[24b] Nevertheless, at this point, a direct link between SEI and LEDC still remains to be established.

In Table 3 the averaged weight retentions of these salts at 400 °C were tabulated. For LMC, LEC, LEDC, and LPDC the remnant after the major decompositions accounted for 42.10%, 28.55%, 35.58%, and 31.35% of the original weight, respectively. Richard et al. once proposed a pathway for the decomposition of lithium alkyl carbonate with Li_2CO_3 as the final product, as shown in Scheme 8.[25] However, our previous study on LMC thermal decomposition has led us to propose a competing mechanism leading to methoxide,[10] which can be generalized to describe both alkyl mono- and dicarbonates as in Scheme 9.

Although lithium methoxide can remain stable up to 500 °C,[26] the other alkoxides containing more organic moieties—especially the dialkoxides from LEDC and LPDC—could further decompose into a more inorganic form before 400 °C. Thus, we believe that a mechanism leading to an "ultimately stable" species should also play a role during the final stages of the thermal chemistry, as shown in Scheme 10.

The above hypothesis seems to be supported by the TGA-FTIR experiments performed on LMC and LEDC, where

SCHEME 10: Continued Thermal Decomposition of Alkoxides Leading to Lithium Oxide

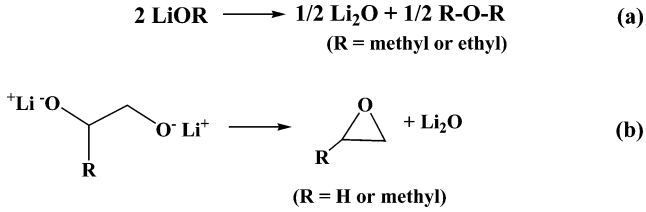

dimethyl ether and ethylene oxide have been detected, respectively.[10,27] To further examine the validity of the above reaction pathways, we used XPS and NMR to conduct a series of chemical analyses on the TGA remnants after the samples were heated to different temperatures as marked by asterisks in Figure 9b. Figures 10a and 10b showed the XPS analyses for LEDC at 160 and 400 °C, in which as a reference the bulk salt before the TGA scan was also shown. Obviously from the C 1s core spectra (Figure 10a), the shifted carbonyl peak at 160 °C does indicate that the pristine LEDC has experienced certain chemistry at the 120 °C event; however, the 290 eV peak, corresponding to the carbonyl in inorganic carbonate, appeared at 400 °C and indicated a complete conversion to Li_2CO_3, thus establishing Scheme 8 as a pathway only initiated at higher temperatures than Scheme 9. The evidence for the subsequent Schemes 9 and 10 comes from the O 1s core spectra (Figure 10b), where the oxygen species corresponding to inorganic oxide (Li_2O) can be distinctly identified in the LEDC sample after being heated to 400 °C. As Li_2CO_3 remains thermally inert up to ∼1000 °C, the detected Li_2O must be produced from alkoxides via Scheme 10. More convincing support for the loss of the alkyl moiety as predicted by Scheme 10 comes from NMR analysis, as shown in the ^{13}C spectra of LEDC in Figure 10c. In the sample treated at 160 °C, the alkoxyl part of the salt ($-O-CH_2-$) was still visible at 62.85 ppm as expected, showing that Scheme 9 might be the only mechanism responsible at this stage. The general pattern of the spectrum remains

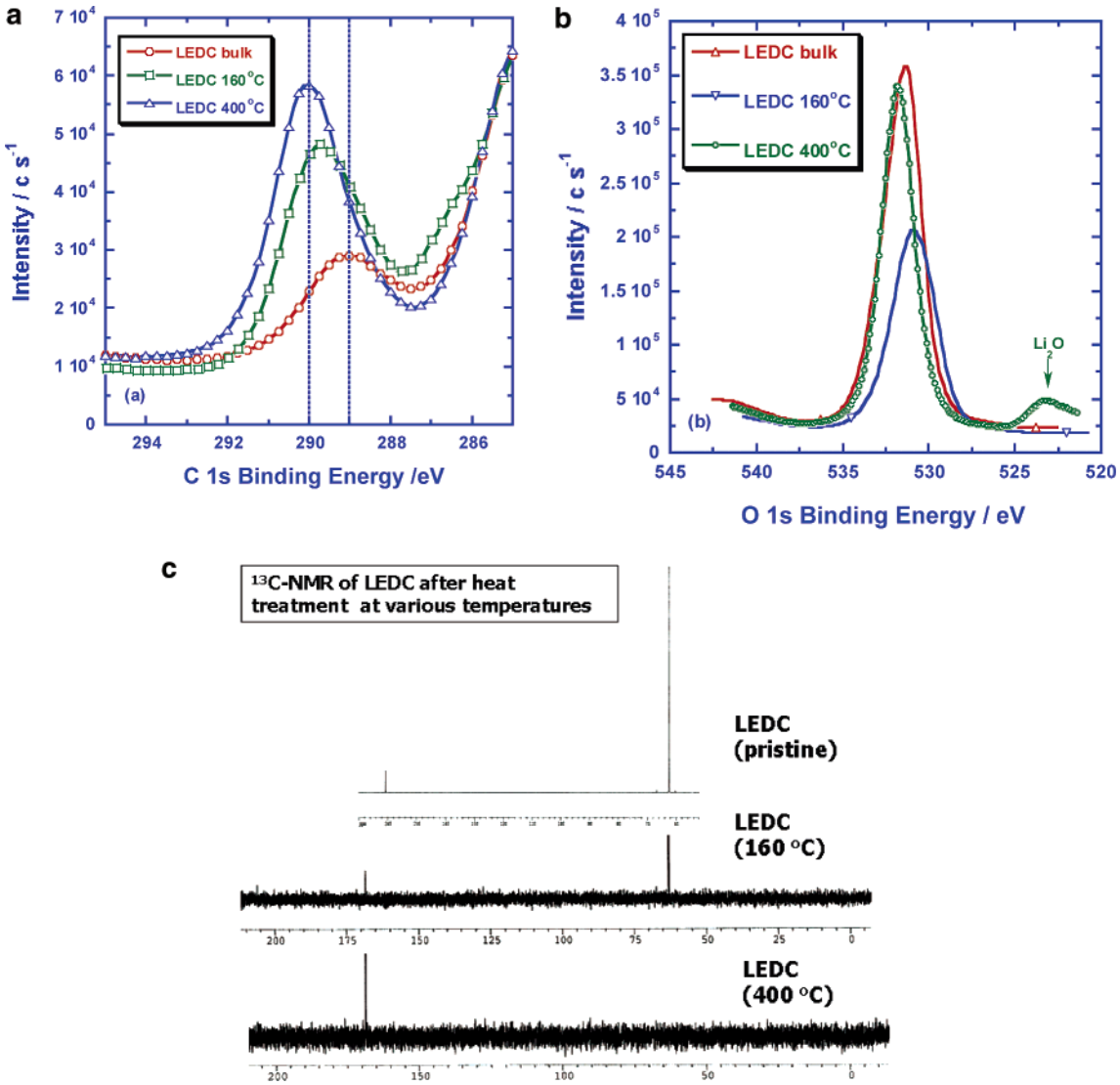

Figure 10. The XPS and NMR analyses on the LEDC samples treated at different temperatures: (a) C 1s, (b) O 1s, and (c) ^{13}C NMR (in D_2O). The peak intensities in parts a and b were normalized against the elemental carbon 1s excitation at 284.86 eV. In all figures the pristine LEDC was also shown as a reference.

similar to that of the pristine salt, as the NMR cannot effctively distinguish the carbonyls of alkyl carbonate and inorganic carbonate salts. However, in the sample treated at 400 °C, the above alkyl moiety entirely vanished, probably in the forms of dialkyl ethers or alkene oxides leaving behind Li_2O (Scheme 10). The only peak detected in this sample at 168.50 ppm should represent the Li_2CO_3 produced through Scheme 8. The parallel XPS and NMR analyses conducted on LPDC yielded similar results.

On the basis of the above information, we draw the conclusion that the thermal decomposition processes of these four lithium alkyl carbonates should consist of two parallel pathways as represented by Schemes 8 and 9, while an additional pathway Scheme 10 should weigh in at higher temperatures consecutive to Scheme 9. This general rationale is consistent with the previous study carried out with on-line TGA-FTIR on LMC.[10] For these four alkyl carbonates, the temperatures at which the above schemes start to exert effects may vary from salt to salt, so does their extent. Figure 11 plotted the weight retentions as predicted by Schemes 8−10 as if they were the sole mechanisms responsible, in comparison with the experimental data. In this manner we wish to show the extent of each scheme in influencing the actual thermal chemistry of these alkyl carbonates. If merely judged by the values of weight retentions, the

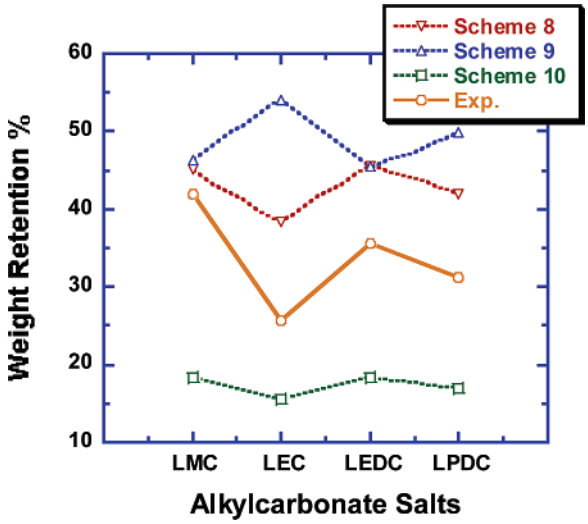

Figure 11. Relatedness of experimental data to the thermal decomposition mechanisms as represented by Schemes 8−10.

experimental data did not demonstrate apparent relevance to any of these mechanisms, an indicator of the absence of any single individual mechanism in absolute dominance. The fact

that the experimental data lie between Schemes 8 and 10 suggested that Schemes 8 and 9 should coexist, considering that Scheme 10 is a continuation of Scheme 9. The experimental weight retentions of LEC, LEDC, and LPDC situate relatively closer to the data as predicted by Scheme 10 than LMC. We attribute this higher relatedness to the lower thermal stability of the corresponding alkoxides of these three alkylcarbonates. However, the general trend of the experimental data varying with salt species roughly matches that of Scheme 8, suggesting that the Li_2CO_3-producing pathway could have higher share in dictating the thermal decomposition of all these salts at the terminal temperature of 400 °C. This may explain why the numerous post-mortem spectroscopic analyses of anode surfaces harvested from aged Li-ion batteries have unanimously identified Li_2CO_3 as the most obvious species.[5,7,21,22] The thermal profiles described above for these four lithium alkyl carbonates have proven useful as references to identify the thermal events of anode surfaces formed in actual Li-ion devices, which will be discussed in our subsequent publications.

Conclusions

A homologous series of alkyl mono- and dicarbonate lithium salts were synthesized, and extensive structural and physicochemical characterizations by means of NMR, FTIR, XRD, XPS, and TGA were carried out. Serving as model references for the frequently proposed electrochemical reduction products in Li-ion batteries, the availability of these compounds in the bulk state makes it possible to understand the fundamental chemistries of SEI in an unprecedented manner. Various chemical mechanisms concerning the stability of these compounds were suggested based on experimental data, and the established spectral and physicochemical database would be of significance to the researchers of Li-ion battery technology.

Acknowledgment. This work is supported by the Office of FreedomCAR and Vehicle Technologies of the U. S. Department of Energy under contract numbers DE-AI01-99EE5061 (ARL) and DE-AC02-05CH11231 (LBNL), respectively. The authors are also grateful to Drs. Yiufai Lam and Yingde Wang of the NMR facility, University of Maryland, for technical support.

References and Notes

(1) Fong, R.; von Sacken, U.; Dahn, J. R. *J. Electrochem. Soc.* **1990**, *137*, 2009
(2) Xu, K. *Chem. Rev.* **2004**, *104*, 4303.
(3) Aurbach, D.; Daroux, M. L.; Faguy, P. W.; Yeager, E. *J. Electrochem. Soc.* **1987**, *134*, 1611.
(4) Aurbach, D.; Gofer, Y.; Ben-Zion, M.; Aped, P. *J. Electroanal. Chem.* **1992**, *339*, 451.
(5) Aurbach, D.; Ein-Eli, Y.; Markovsky, B.; Zaban, A.; Luski, S.; Carmeli, Y.; Yamin, H. *J. Electrochem. Soc.* **1995**, *142*, 2882.
(6) Ein-Eli, Y. *Electrochem. Solid-State Lett.* **1999**, *2*, 212.
(7) Zhuang, G. V.; Ross, P. N., Jr. *Electrochem. Solid-State Lett.* **2003**, *6*, A136.
(8) (a) Xu, K.; Lee, U.; Zhang, S.; Wood, M.; Jow, T. R. *Electrochem. Solid-State Lett.* **2003**, *6*, A144. (b) Xu, K.; Lee, U.; Zhang, S.; Allen, J. L.; Jow, T. R. *Electrochem. Solid-State Lett.* **2004**, *7*, A273.
(9) Zhuang, G. V.; Xu, K.; Yang, H.; Jow, T. R.; Ross, P. N., Jr. *J. Phys. Chem. B* **2005**, *109*, 15767.
(10) Zhuang, G. V.; Yang, H.; Ross, P. N., Jr.; Xu, K.; Jow, T. R. *Electrochem. Solid-State Lett.* **2006**, *9*, A64.
(11) Gireaud, L.; Grugeon, S.; Laruelle, S.; Pillard, S.; Tarascon, J.-M. *J. Electrochem. Soc.* **2005**, *152*, A850.
(12) Dedryvère, R.; Gireaud, L.; Grugeon, S.; Laruelle, S.; Tarascon, J.-M.; Gonbeau, D. *J. Phys. Chem. B* **2005**, *109*, 15868.
(13) Zhuang, G. V.; Xu, K.; Jow, T. R.; Ross, P. N., Jr. *Electrochem. Solid-State Lett.* **2004**, *7*, A224.
(14) Werner, P.-E.; Eriksson, L.; Westdahl, M. *J. Appl. Crystallogr.* **1985**, *18*, 367.
(15) Dumas, J.; Peligot, E. *Justus Liebigs Annalen der Chemie*, **1840**, *35*, 283.
(16) Simons, W. W. *The Sadler Handbook of Proton NMR Spectra Index*; Sadler Laboratory: Philadelphia, PA, 1978.
(17) Reddy, V. P.; Smart, M. C.; Chin, K. B.; Ratnakumar, B. V.; Surampudi, S.; Hu, J.; Yuan, P.; Prakash, G. K. S. *Electrochem. Solid-State Lett.* **2005**, *8*, A294.
(18) de Wolff, P. M. *J. Appl. Crystallogr.* **1968**, *1*, 108.
(19) de Wolff, P. M. *J. Appl. Crystallogr.* **1972**, *5*, 243.
(20) (a) Tasaki, K. *J. Electrochem. Soc.* **2002**, *149*, A418. (b) Tasaki, K.; Nakamura, S. *J. Electrochem. Soc.* **2001**, *148*, A984.
(21) Aurbach, D.; Ein-Eli, Y. *J. Electrochem. Soc.* **1995**, *142*, 1746.
(22) Kanamura, K.; Tamura, H.; Shiraishi, S.; Takehara, Z. *J. Electrochem. Soc.* **1995**, *142*, 340.
(23) (a) Christe, K. O.; Dixon, D. A.; McLemore, D.; Wilson, W. W.; Sheehy, J. A.; Boatz, J. *J. Fluorine Chem.* **2000**, *101*, 151. (b) Sloop, S. E.; Pugh, J. K.; Wang, J. B.; Kerr, J. B.; Kinoshita, K. *Electrochem. Solid-State Lett.* **2001**, *4*, A42.
(24) (a) Du Pasquier, A.; Disma, F.; Bowmer, T.; S. Gozdz, A.; Amatucci, G.; Tarascon, J. M. *J. Electrochem. Soc.* **1998**, *145*, 472. (b) Maleki, H.; Deng, G.; Anani, A.; Howard, J. *J. Electrochem. Soc.* **1999**, *146*, 3224.
(25) Richard, M. N.; Dahn, J. R. *J. Electrochem. Soc.* **1999**, *146*, 2068.
(26) Material Safety Data Sheet; Sigma-Aldrich, Oct 2005.
(27) Zhuang, G. V.; Ross, P. N., Jr. Unpublished work.